Proceedings of ICFDP 8:
Eighth International Congress of Fluid Dynamics & Propulsion
December 14-17, 2006, Sharm El-Shiekh, Sinai, Egypt
ICFDP8-EG-155

Force Convection in Channel Filled Partially with Porous Medium Including the Effects of Thermal Conductivity

Abdulnannan A. Saati

Dept. of Mechanical Engineering,
Umm Al-Qura University,
Makkah,
Saudi Arabia

ABSTRACT

This paper presents numerical investigations for heat transfer enhancement in a channel partially filled with porous material. In fact, the porous material is attached to the inner side of the channel wall. Force turbulent flow is assumed and the effects of thermal conductivity and Darcy (permeability) on the rate of heat transfer, is also investigated. In the analysis, developing and fully developed flow conditions are considered. Moreover, numerical results obtained by utilizing low Reynolds number (LRN) $k-\varepsilon$ model are computed and analyzed in details.

NOMENCLATURE

c_p	Specific heat at constant pressure ($J/kg\,K$)
Da	Darcy number K/H^2
g	Acceleration due to gravity (m/s^2)
H	Half of the channel height (m)
hp	height of the porous material
K	Permeability (m^2)
k	kinetic energy of turbulent (m^2/s^2)
k_{eff}	Effective thermal conductivity $k_{eff} = \lambda_m / \lambda$
k_{in}	inlet kinetic energy of turbulent (m^2/s^2)
k_w	kinetic energy near – wall(m^2/s^2)
L	length of the channel (m)
Nu	local Nusselt number
Nu_{av}	average Nusselt number
p	pressure (Pa)
Pr	Prandtl number, $\mu c_p / \lambda$
Pr_t	Turbulent Prandtl number $k^2/\nu\varepsilon$
Re	U_{in} 2 H/ν
T	Temperature (K)
T_{in} , T_w	inlet and wall Temperatures
U, V	velocity components
U_{in}	inlet velocity
x , y	Coordinates
ε	dissipation rate of turbulent

	kinetic energy (m^2/s^3)
ε_{in}	Inlet dissipation rate
ε_w	dissipation rate of turbulent kinetic energy near –wall
η	dimensionless transversal coordinate (*y/H*)
λ	Thermal conductivity (*W/mK*)
λ_m	Thermal conductivity of the material (*W/mK*)
μ	Dynamic viscosity (kg/m s)
μ_t	turbulent viscosity (kg/m s)
ν	Kinematic viscosity (m^2/s)
ρ	density (kg/m^3)
σ_k , σ_ε	Turbulent Prandtl number in $k-\varepsilon$ model equations
ξ	dimensionless axial coordinate (*x/L*)

1- Introduction

The employment of different types of porous materials in the force convection Heat transfer enhancements have been extensively investigated due to its wide range of engineering applications, such as in heat exchangers, Boilers, condensers, cooling of electronics, solar collectors, etc. There are many advantages of using porous medium techniques such as: a) When the thermal conductivity of the porous material is higher than the thermal conductivity of the fluid, the rate of heat transfer and the convective heat transfer coefficient are increased for the systems filled or partially filled with porous material more than the system without porous material. b) The changing of the geometrical characteristics and the position of the porous material also improve the enhancement of the rate of heat transfer e.g. , in channel flow the rate of heat transfer with partial filling system is higher than the system filled completely with porous material.

Partial filling has many advantages such as: decreasing the pressure drop, and reducing the boundary layer thickness which enhances the rate of heat transfer in comparison with channel completely filled with porous material. In fact, the development of heat transfer by using porous material have been investigated for different engineering and industrial applications for external and internal flows. For instance, Mohamad [10] developed a solar air heater with the porous medium to enhance the rate of heat transfer and reduce the heat losses to the ambient. Jang and Chen [7] studied numerically force flow in a channel partially filled with a porous medium by adopting the Darcy-Brinkman-Forchheimer model with thermal dispersion effects. Chikh *et al*. [5,6] were presented analytical solutions for a fully developed flow in annulus configuration partially filled with porous medium. The transient solution for annulus flow and forced convection behavior of a flow in parallel plate channels with a porous material have been studied by Al-Nimr and Alkann [2], Alkam *et al*. [4] and abu-Hijleh and Al-Nimr [1]. The force convection flow in concentric annuli partially filled with porous material either on the inner or on the outer cylinder, and on both sides of the inner cylinder were numerically investigated by Al-Nimr and Alkam [2] and Alkam and Al-Nimr [3]. They concluded that the Nusselt number was increased up to 12 times for these cases than that for the clear annuli case. The results also showed optimum thicknesses

of the porous material that yield maximum rate of heat transfer. Mohamad [11] numerically investigated the heat transfer for laminar flow in pipe or channel partially or fully filled with porous material at the core of the channel and the wall is kept at a constant and uniform heat flux. The result showed that the thermal entrance length reduced by more than 50% and the rate of heat transfer increased for channel with partially filled.

Recently, studies are conducted related to turbulent flow in domains that are partially filled with porous material. Zhu and Kuznetson [17] investigated the force convection in composite parallel plate channel based on the assumption that the flow domain is divided into two regions, the clear fluid region where the flow is assumed to be turbulent which is solved by utilizing a $k-\varepsilon$ model, and porous region where the flow is assumed to be laminar. For the same problem Silva and de Lemos [16] and de Lemos [8] investigated the behavior of turbulent flow across the interface between the porous layer and the clear region.

In the present work, the study of turbulent flow in a channel partially filled with porous layer is considered numerically for constant wall temperature boundary conditions. The constant wall temperature condition is encountered in many industrial heat exchanger applications. Simulations are performed for turbulent flow by adopting Rahman's model (Rahman and Siikonen [14]), which is the best among different models for forced convection. The main objective of this work is to analyze the heat transfer enhancement for partially filled channels with porous medium. The effects of thermal conductivity for different Darcy (permeability) on the rate of heat transfer are discussed and conditions for optimal operating condition are also suggested.

2- Problem definition

The schematic diagram of the problem is shown in Fig. 1. Turbulent natural convection in channel is partially filled and attached to the inner side of the channel wall. An air stream with uniform velocity and temperature is considered at the inlet to the channel. The wall temperature of the channel is fixed, and is higher than the inlet temperature.

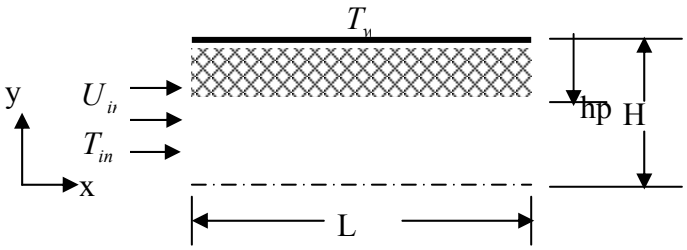

Fig. 1. Schematic diagram of the problem

3- Governing Equations

Steady and incompressible two-dimensional flow, was assumed. Reynolds-averaged Navier-Stokes (RANS) equations, including the equation of the kinetic energy k and its dissipation rate ε are assume valid (Mohamad [9]). It is also assumed that all physical properties are neither temperature nor pressure dependent, and the buoyancy effects are negligible. The governing equation may be written in the following form:

Continuity:

$$\frac{\partial}{\partial x}(\rho U)+\frac{\partial}{\partial y}(\rho V)=0 \qquad (1)$$

X-momentum:

$$\frac{\partial}{\partial x}(\rho UU)+\frac{\partial}{\partial y}(\rho VU)=-\frac{\partial p}{\partial x}+$$
$$\frac{\partial}{\partial x}\left[(\mu+\mu_t)\frac{\partial U}{\partial x}\right]+\frac{\partial}{\partial y}\left[(\mu+\mu_t)\frac{\partial U}{\partial y}\right]$$
$$-\frac{2}{3}\rho\frac{\partial k}{\partial x}-f\frac{\mu+\mu_t}{K}U \qquad (2)$$

Y-momentum:

$$\frac{\partial}{\partial x}(\rho UV)+\frac{\partial}{\partial y}(\rho VV)=-\frac{\partial p}{\partial y}+$$
$$\frac{\partial}{\partial x}\left[(\mu+\mu_t)\frac{\partial V}{\partial x}\right]+\frac{\partial}{\partial y}\left[(\mu+\mu_t)\frac{\partial V}{\partial y}\right]$$
$$-\frac{2}{3}\rho\frac{\partial k}{\partial y}-f\frac{\mu+\mu_t}{K}V \qquad (3)$$

Energy:

$$\frac{\partial}{\partial x}(\rho UT)+\frac{\partial}{\partial y}(\rho VT)=\frac{\partial}{\partial x}\left[\left\{\frac{\lambda}{C_p}+\frac{\mu_t}{\mathrm{Pr}_t}\right\}\frac{\partial T}{\partial x}\right]$$
$$+\frac{\partial}{\partial y}\left[\left\{\frac{\lambda}{C_p}+\frac{\mu_t}{\mathrm{Pr}_t}\right\}\frac{\partial T}{\partial y}\right] \qquad (4)$$

The turbulence kinetic energy, k,

$$\frac{\partial}{\partial x}(\rho Uk)+\frac{\partial}{\partial y}(\rho Vk)=\frac{\partial}{\partial x}\left[\left(\mu+\frac{\mu_t}{\sigma_k}\right)\frac{\partial k}{\partial x}\right]$$
$$+\frac{\partial}{\partial y}\left[\left(\mu+\frac{\mu_t}{\sigma_k}\right)\frac{\partial k}{\partial y}\right]+P-\rho\varepsilon \qquad (5)$$

The dissipation rate (ε):

$$\frac{\partial}{\partial x}(\rho U\varepsilon)+\frac{\partial}{\partial y}(\rho V\varepsilon)=$$
$$\frac{\partial}{\partial x}\left[\left(\mu+\frac{\mu_t}{\sigma_\varepsilon}\right)\frac{\partial \varepsilon}{\partial x}\right]+\frac{\partial}{\partial y}\left[\left(\mu+\frac{\mu_t}{\sigma_\varepsilon}\right)\frac{\partial \varepsilon}{\partial y}\right]$$
$$+(C_1P-C_2\rho\varepsilon+E_\varepsilon)/T_t+\prod_\varepsilon \qquad (6)$$

Where, f is set to unity for flow in porous medium and to zero for flow in region without porous material. The right-hand-side terms in equations (5) and (6) are the production, the dissipation, the diffusion and an additional source term, respectively. The LRN $k-\varepsilon$ model used in this work is the most recent model proposed by Rahman and Siikonen [14]. Where the turbulent production term by shear stresses P may be modeled as:

$$P=\mu_t\left[2\left\{\left\{\frac{\partial U}{\partial x}\right\}^2+\left\{\frac{\partial V}{\partial y}\right\}^2\right\}+\left[\frac{\partial U}{\partial y}+\frac{\partial V}{\partial x}\right]^2\right] \qquad (7)$$

The functions for the LRN turbulence models has been described in detail in a different place (Rahman and Siikonen [14]). The turbulence time scale and the model constants are evaluated as:

$$T_t=\sqrt{\frac{k^2}{\varepsilon^2}+2\frac{\nu}{\varepsilon}} \qquad (8)$$

where the damping function f_μ is chosen to be a function of R_λ, which is given by

$$f_\mu=f_\lambda+C_\nu(1-f_\lambda),$$
$$R_\lambda=\sqrt{\frac{C_\mu K_T}{\nu\eta}},$$
$$f_\lambda=\tanh\left[C_\lambda R_\lambda(1+R_\lambda)\right], \qquad (9)$$
$$K_T=U\bullet U/2+k, \qquad C_\mu=0.09$$

Where: $C_\lambda=\beta C_\mu^{\,C_2}$, $\beta=C_\nu T_t\eta$ and

$$\eta=\max(S,W), \qquad S=\sqrt{(2S_{ij}S_{ij})},$$
$$W=\sqrt{(2W_{ij}W_{ij})}$$
$$C_\nu=\frac{1}{2\left(1+T_t\sqrt{S^2+W^2}\right)}$$

The mean strain rate and the mean velocity tensors S_{ij} and W_{ij} are defined as:

$$S_{ij} = \frac{1}{2}\left(\frac{\partial U_i}{\partial x_j} + \frac{\partial U_j}{\partial x_i}\right)$$

$$W_{ij} = \frac{1}{2}\left(\frac{\partial U_i}{\partial x_j} - \frac{\partial U_j}{\partial x_i}\right) \qquad (10)$$

The turbulence Prandtl numbers σ_k and σ_ε are modeled as:

$$\sigma_\varepsilon = \sqrt{2}\left[4C_\nu + f_\sigma\right], \quad \sigma_k = \frac{\sigma_\varepsilon}{\left[1 - C_\nu f_\sigma\right]} \qquad (11)$$

Where $f_\sigma = f_\mu / (\sqrt{\beta} + f_\mu^3)$ and

$$C_1 = 1 + \beta, \qquad C_2 = 1.33\ C_1 \qquad (12)$$

The extra source term in the dissipation rate ε equation is written as:

$$E_\varepsilon = 2\frac{\mu_T}{T_t}\max\left(\frac{\partial(k/\varepsilon)}{\partial x_j}\frac{\partial k}{\partial x_j}, 0\right) \qquad (13)$$

and the pressure diffusion term can be written as:

$$\prod_\varepsilon = -\frac{1}{2}\frac{\partial}{\partial x_j}\left[\frac{\rho k}{2 + R_t}\frac{\partial k}{\partial x_j}\right] \qquad (14)$$

***Nusselt number*:**

Nusselt Number Calculations

The Nusselt number for a pipe can be calculated as:

$$Nu = \frac{4\dfrac{\partial T}{\partial y}H}{T_w - T_m} \qquad (15)$$

where T_m stands for the fluid bulk temperature inside the channel.

The bulk temperature for flow in a channel can be calculated as:

$$T_m = \frac{\int_0^H U\,T\ dy}{\int_0^H U\ dy} \qquad (16)$$

***Boundary conditions*:**

Symmetric boundary conditions are adopted for y=0, i.e., *V=0* and the gradients of *U*, *T*, *k* and ε in the y-direction set to zero. No slip condition is assumed for *y=H* and $0 < x < L$, i.e., the velocities are assumed to be zero ($U = V = 0$) and $T = T_w$. The *V* velocity component is set to zero, $U = U_{in}$, $T = T_{in}$, $k = k_{in}$ and $\varepsilon = \varepsilon_{in}$ at *x-0*. For *x=L*, the gradients of the variables in x-direction are set to zero. The boundary conditions for the turbulence kinetic energy *k* and its dissipation ε at the solid walls (*y=H*) are given by equation (17). The grid system must be fine enough in order to produce the near – wall limiting performance

$$k_w = 0\ , \qquad \varepsilon_w = 2\nu\left(\frac{\partial\sqrt{k}}{\partial y}\right)^2 \qquad (17)$$

3- Method of Solution

Control volume, finite-difference technique was used to solve the model equations with appropriate boundary conditions. The SIMPLER algorithm was employed to solve the equations in primitive variables and it is discussed in details by Patankar [12]. The governing equations are converted to a system of algebraic equations through an appropriate integration over each control volume of the domain and finite-difference approximation. The algebraic equations are solved using line-by-line iterative method coupled with an additive correction procedure to help speed the convergence. The method solves a line of nodes using the tri-diagonal matrix inversion algorithm and sweeps the domain of the integration in different directions along the x- and y-axis. Second order central-difference discretization of the diffusive-advective flux is used for the spatial derivatives. Velocity components and kinetic energy are under-relaxed by a factor of 0.7, and the temperature by a factor of 0.9. The criteria for convergence are to conserve

mass, momentum and energy globally and locally and to ensure convergence of pre-selected dependent variables to constant values within machine error. In order to insure that the results are grid size independent, different meshes are tested namely, 201×101, 241×121, 281×141 and 301×161. For most calculations, 9000 iterations are sufficient to get convergent solution for 281×141 grids.

4- Results and discussions

Calculations are conducted in the half height of the channel, where the length of the computation domain is 20 m, and the channel half height H = 0.2 m. The influences of the effective thermal conductivity (k_{eff}) and porous permeability (*Da* number) are numerically studied. The investigated Reynolds number is 5000 with inlet temperature, $T_{in} = 30\ ^{\circ}C$, and wall temperature, $T_w = 70\ ^{\circ}C$.

The fully developed velocity profile at $Da = 10^{-4}$ for range of the porous layer thicknesses (hp = 0.2, 0.4 and 0.6) have been investigated for different effective thermal conductivity ($k_{eff} = 1,5,10\ and\ 50$). The result shows that the flow mostly channels at the center, where it could be negligible through the porous material. It also shows that there is no influence of k_{eff} on the flow as shown in Fig. 2 at $k_{eff} = 1\ and\ 10$.

Figures 3 illustrates the fully developed velocity profiles at porous layer thickness hp = 0.6 and the range of Darcy number ($Da = 10^{-2}, 10^{-3},\ 10^{-4}$). Due to moderate permeability of the porous medium, the flow rate in the porous medium decreases as *Da* decreases, and it can be neglected for $Da \le 10^{-4}$.

Nusselt number variation along the channel at $Da = 10^{-2}, 10^{-3}, 10^{-4}$, and different porous layer thickness (*hp* = 0.2, 0.4 & 0.6) with different effective thermal conductivity (k_{eff}) are shown in Fig. 4 - 12. The Nusselt number variations for different k_{eff} is significantly large and greater than the flow without porous material in the developed flow region ($\xi \le 0.5$), and the difference exponentially decreases and becomes close to the clear flow case at $\xi \ge 0.5$. Figure 5 – 9 show the Nusselt number less than the clear flow case for $k_{eff} = 1$ only, but the *Nu* is maximum for $k_{eff} = 50$ at the developed flow region ($\xi \le 0.5$)and then exponentially decreases and becomes less than the clear flow case. Figure 10 – 12 show the Nusselt number for all cases with porous medium is increased in comparison with the clear flow case.

Figures 13 - 15 present the influence of both effective thermal conductivity and *Da* for different porous layer thickness on the average Nusselt number, Nu_{av}. The average Nusselt number increases as k_{eff} increases. The average Nusselt number is maximum for hp = 0.2 and k_{eff} up to 10. The difference in the average Nusselt number can be negligible for all porous layer thickness (hp) when k_{eff} is 50 as shown in Fig. 13. On the other hand, the average Nusselt number is maximum when hp = 0.6 and $Da = 10^{-3}, 10^{-4}$ as shown in Fig. 14 & 15. The difference in the average Nusselt number can be negligible for hp = 0.2, 0.4 and

$Da = 10^{-2}, 10^{-4}$ as show in Fig. 13 and 15.

It should be mentioned that the pressure drops increases as Darcy number decreases, especially for high velocity flows and low Da number, the pressure drop may become significantly high and increase in Nu number compensated by the pumping power. However, the experimental results of Pavel and Mohamad [13], showed that the pressure drop is not that significant for Da > 10^{-2}, and the numerical result of Saati and Mohamad [15], shows the influence of porous layer (hp) on the rate of heat transfer and the pressure drop but the present work shows that there is no influence of the effective thermal conductivity (k_{eff}) on the pressure drop. It is recommended to use high preamble porous media and k_{eff} for heat transfer enhancement.

5- Conclusion

Heat transfer enhancement in a channel partially filled with porous material is presented for a range of effective thermal conductivity (k_{eff}) and Darcy number. It is found that the flow rate in the porous medium decreases, as *Da* decreases, and the flow can be negligible for, $Da \le 10^{-4}$, and it also, found that the rate of heat transfer increased as effective thermal conductivity increased. The maximum rate of heat transfer take places at porous layer thickness about hp = 0.6 and for $Da = 10^{-3}, 10^{-4}$. But for Da=10^{-2} the maximum rate of heat transfer occur at porous layer thickness about hp = 0.2. At last the result show that the enhancement of heat transfer which is using porous material should be limited to high permeable media to avoid high pressure drop in the system.

Reference

[1] Abu-Hijleh, B.A, and Al-Nimr, M.A., 2001. The effect of the local inertial term on the fluid flow in channel partially filled with porous material, International Journal of Heat and Mass Transfer, 44, 1565-1572.

[2] Al-Nimr, M.A. and Alkam, M.K., 1997. Unsteady non-Darcian forced convection analysis in an annulus partially filled with a porous material, ASME Journal of Heat Transfer, 119, 799-804.

[3] Alkam, M.K. and Al-Nimr, M.A., 1999. Improving the performance of double-pipe heat exchanger by using porous substrates, International Journal of Heat and Mass Transfer, 42, 3609-3618.

[4] Alkam, M.K., Al-Nimr, M.A. and Hamdan, M.O., 2001. Enhancing heat transfer in parallel-plate channels by using porous inserts, International Journal of Heat and Mass Transfer 44, 931-938.

[5] Chikh, S., Boumedien, A., Bouhadef, K. and Lauriat, G., 1995-a. Analytical solution of non-Darcian forced convection in an annular duct partially filled with a porous medium, International Journal of Heat and Mass Transfer, 38, 1543-1551.

[6] Chikh, S., Boumedien, A., Bouhadef, K. and Lauriat, G., 1995-b. Non-Darcian forced convection analysis in an annular duct partially filled with a porous medium, Numerical Heat Transfer 28, 707-722.

[7] Jang, J.Y. and Chan, J.L., 1992. Forced convection in a parallel plate channel partially filled with a high porosity medium,

International Communications in Heat Mass Transfer 19, 263-273.

[8] de Lemos M.J.S., 2005. Turbulent kinetic energy distribution across the interface between a porous medium and clear region, International Journal Heat and Mass Transfer 32, 107-115.

[9] Mohamad, A.A., 1992. Mixed convection in lid-driven shallow cavities, PhD thesis, School of Mechanical Engineering, Purdue University, USA.

[10] Mohamad, A.A., 1997. High efficiency solar air heater, Solar Energy 60**,** 71-76

[11] Mohamad, A.A., 2003. Heat transfer enhancements in heat exchangers fitted with porous media, Part I: constant wall temperature, International Journal of Thermal Sciences 42**,** 385-395.

[12] Patankar, S.V., 1980. Numerical Heat Transfer and Fluid Flow. McGraw-Hill, New York.

[13] Pavel, B.I. and Mohamad, A.A., 2004. An experimental and numerical study on heat transfer enhancement for gas heat exchangers fitted with porous media, International Journal Heat and Mass Transfer 47, 4939-4952.

[14] Rahman, M.M. and Siikonen, T. 2005. Low Reynolds number $k-\varepsilon$ model for near-wall flow. International Journal for Numerical methods in Fluids, (in press).

[15] Saati, A. and Mohamad, A.A., "Heat Transfer Enhancement in a composite parallel plate channel: Utilizing low Reynolds number $k-\varepsilon$ model", Journal of Porous Media, **Submitted in 2005**

[16] Silva, R.A. and de Lemos, M.J.S., 2003. Turbulent flow in a channel occupied by a porous layer considering the stress jump at the interface, International Journal Heat and Mass Transfer, 46,5113-5121.

[17] Zhu, J. and Kuznetsov, A.V., 2005. Force convection in composite parallel plate channel: modeling the effect of interface roughness and turbulence utilizing a $k-\varepsilon$ model, International Communications in Heat and Mass Transfer 32, 10-18.

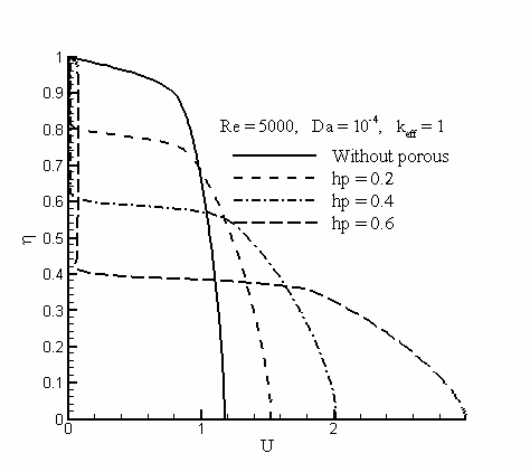

(a)

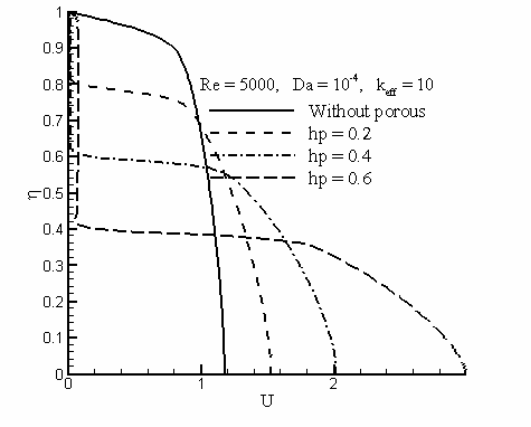

(b)

Fig.2 Fully developed velocity profile for different porous material thickness hp at Re=5000 and $Da = 10^{-4}$ & $k_{eff} = 1 \; and \; 10$.

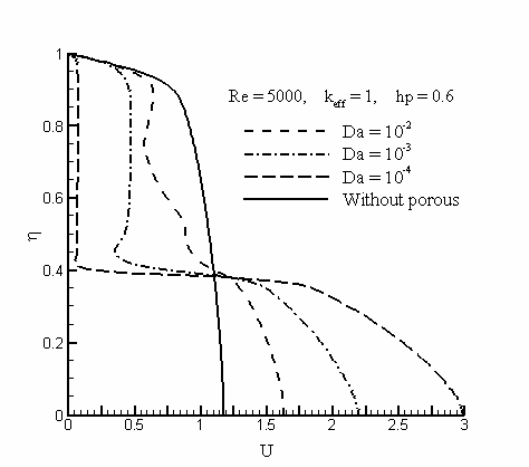

Fig. 3 Fully developed velocity profile for different Darcy number, with Re=5000 and porous layer thickness hp = 0.6 and $k_{eff} = 1$.

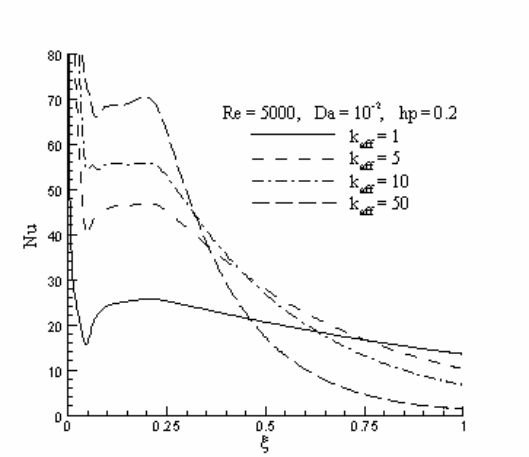

Fig. 4 Influence of the effective thermal conductivity (k_{eff}) on the local Nusselt number at Re=5000, $Da = 10^{-2}$ and hp = 0.2.

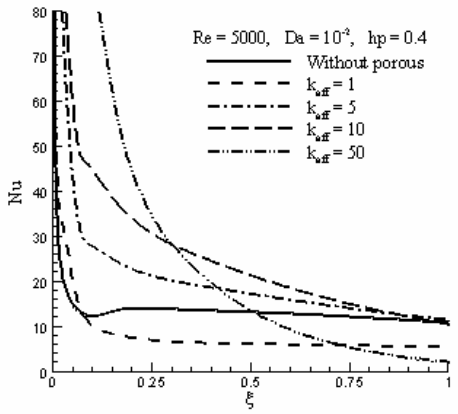

Fig. 5 Influence of the effective thermal conductivity (k_{eff}) on the local Nusselt number at Re=5000, $Da = 10^{-2}$ and hp = 0.4.

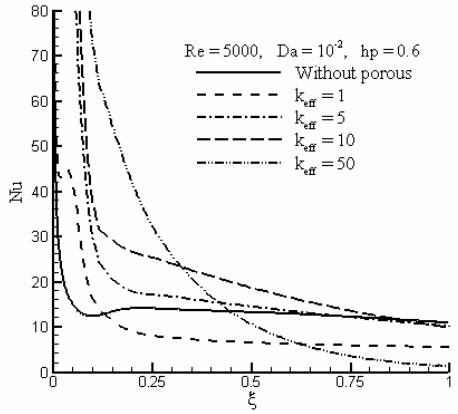

Fig. 6 Influence of the effective thermal conductivity (k_{eff}) on the local Nusselt number at Re=5000, $Da = 10^{-2}$ and hp = 0.6.

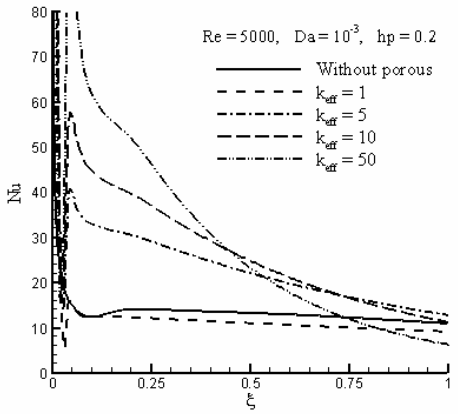

Fig. 7 Influence of the effective thermal conductivity (k_{eff}) on the local Nusselt number at Re=5000, $Da = 10^{-3}$ and hp = 0.2.

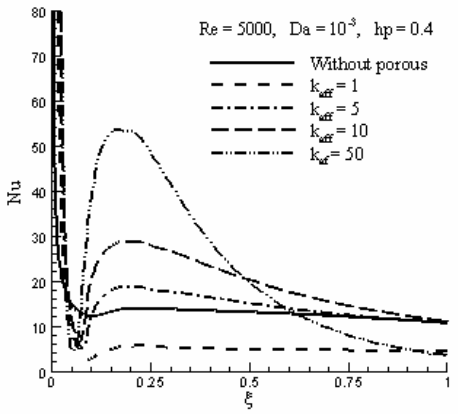

Fig. 8 Influence of the effective thermal conductivity (k_{eff}) on the local Nusselt number at Re=5000, $Da = 10^{-3}$ and hp = 0.4.

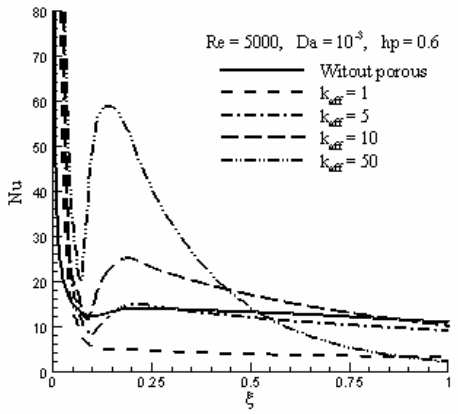

Fig. 9 Influence of the effective thermal conductivity (k_{eff}) on the local Nusselt number at Re=5000, $Da = 10^{-3}$ and hp = 0.6.

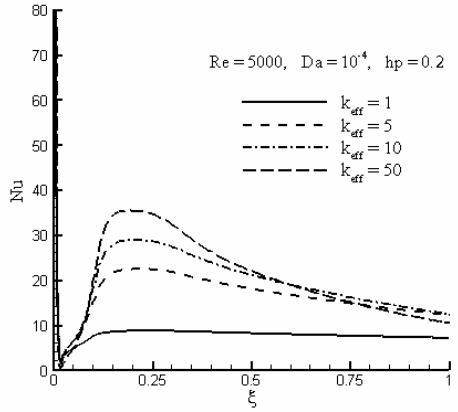

Fig. 10 Influence of the effective thermal conductivity (k_{eff}) on the local Nusselt number at Re=5000, $Da = 10^{-4}$ and hp = 0.2.

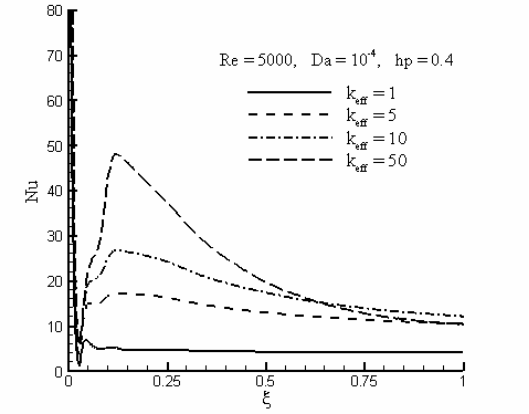

Fig. 11 Influence of the effective thermal conductivity (k_{eff}) on the local Nusselt number at Re=5000, $Da = 10^{-4}$ and hp = 0.4.

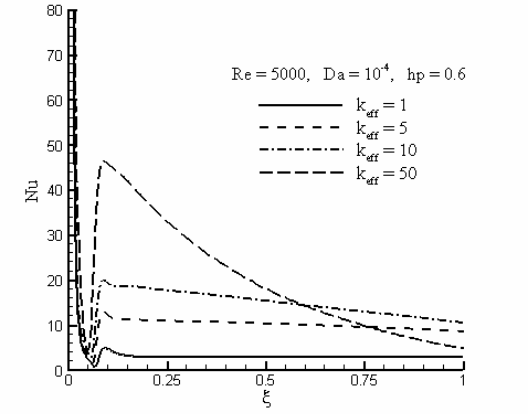

Fig. 12 Influence of the effective thermal conductivity (k_{eff}) on the local Nusselt number at Re=5000, $Da = 10^{-4}$ and hp = 0.6.

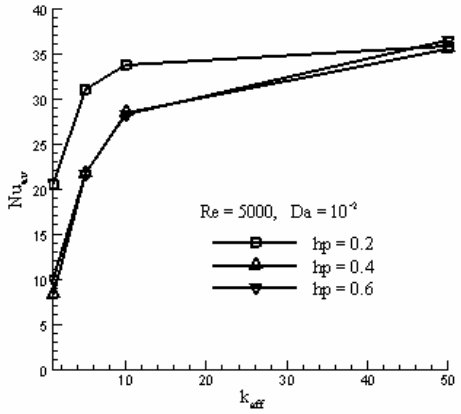

Fig. 13 Average Nusselt number for fully developed channel as function of the effective thermal conductivity (k_{eff}) for different porous layer thickness (hp) with Re=5000 and Darcy number $Da = 10^{-2}$.

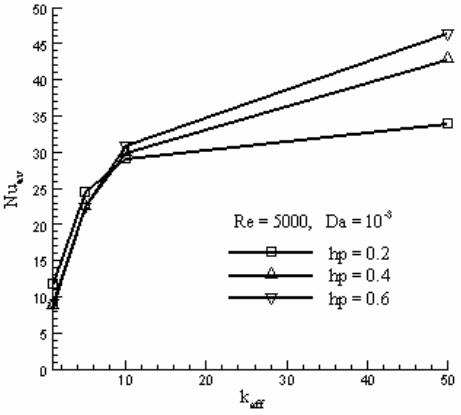

Fig. 14 Average Nusselt number for fully developed channel as function of the effective thermal conductivity (k_{eff}) for different porous layer thickness (hp) with Re=5000 and Darcy number $Da = 10^{-3}$.

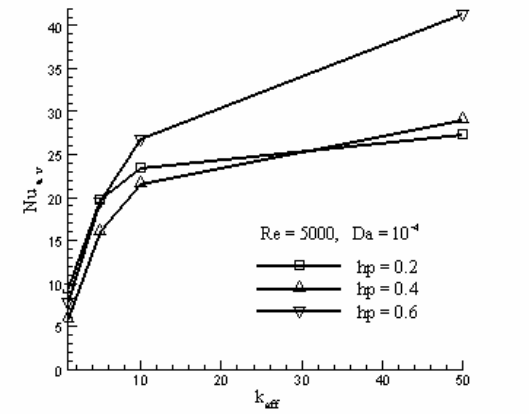

Fig. 15 Average Nusselt number for fully developed channel as function of the effective thermal conductivity (k_{eff}) for different porous layer thickness (hp) with Re=5000 and Darcy number $Da = 10^{-4}$.